

# NJC

New Journal of Chemistry

Accepted Manuscript

A journal for new directions in chemistry

This article can be cited before page numbers have been issued, to do this please use: C. Ji, Y. Deng, H. Yuan, Y. Wu and W. Yuan, *New J. Chem.*, 2020, DOI: 10.1039/D0NJ02114H.



This is an Accepted Manuscript, which has been through the Royal Society of Chemistry peer review process and has been accepted for publication.

Accepted Manuscripts are published online shortly after acceptance, before technical editing, formatting and proof reading. Using this free service, authors can make their results available to the community, in citable form, before we publish the edited article. We will replace this Accepted Manuscript with the edited and formatted Advance Article as soon as it is available.

You can find more information about Accepted Manuscripts in the [Information for Authors](#).

Please note that technical editing may introduce minor changes to the text and/or graphics, which may alter content. The journal's standard [Terms & Conditions](#) and the [Ethical guidelines](#) still apply. In no event shall the Royal Society of Chemistry be held responsible for any errors or omissions in this Accepted Manuscript or any consequences arising from the use of any information it contains.

Journal Name

ARTICLE

## Hypoxia and temperature dually responsive random copolymers: facile synthesis, self-assembly and controlled release of drug

 Chenming Ji<sup>a</sup>, Yinlu Deng<sup>a</sup>, Hua Yuan<sup>a\*</sup>, Yongzhen Wu<sup>b\*</sup> and Weizhong Yuan<sup>a\*</sup>

 Received 00th January 20xx,  
Accepted 00th January 20xx

DOI: 10.1039/x0xx00000x

www.rsc.org/

Amphiphilic random copolymers poly(isopropylacrylamide-co-acrylic acid-co-2-nitroimidazole acrylate) (P(NIPAM-co-AA-co-NIA)) with different contents of 2-nitroimidazole (NI) group were facilely synthesized through RAFT and EDC reactions. These random copolymers self-assembled into spherical micelles at room temperature through dialysis method. NI groups exhibited stimulus responsiveness under hypoxia condition. The hydrophobicity-hydrophilicity transformation could be realized through the change of NI groups into aminoimidazole (AI) groups. Moreover, NIPAM segments endowed the copolymers with thermo-responsive property. In addition, the content of NI group in the copolymers would influence the hydrophilic-hydrophobic equilibrium of the copolymers, and resultingly generated an obvious effect on the self-assembly behaviour of the copolymers and the morphologies of the self-assemblies. The micelles or vesicles can be used as the drug carriers to realize the controlled release of doxorubicin (DOX). The *in vitro* cell viability study of the DOX-loaded self-assemblies indicated the cytotoxicities under hypoxic condition were much higher than those under normoxic condition. Moreover, the drug release behaviors also could be adjusted by changing the temperatures. Therefore, these random copolymers are expected to be the multifunctional and smart carrier for the elimination of cancer cells.

### Introduction

As the novel and smart polymeric materials, hypoxia-responsive polymers have attracted considerable interests owing to their promising applications in the therapic fields of hypoxia-associated diseases including cancer, vascular diseases, anemia, cardiomyopathy and rheumatoid arthritis and so on.<sup>1-10</sup> The nitroaromatic and azobenzene derivatives are two commonly used hypoxia-responsive substances which could be introduced to polymeric chains to construct hypoxia-responsive copolymers.<sup>11-16</sup> As for the nitroaromatic derivatives, the hydrophobic-to-hydrophilic transformation can be completed resulting from the conversion of nitro groups to amino groups under hypoxic conditions. Moreover, the nitroaromatic groups could be facilely linked to the backbones of polymers to construct hypoxia-responsive polymeric materials under mild conditions.<sup>17, 18</sup> Among them, 2-nitroimidazole (NI) groups are important and typical hypoxia-sensitive groups and can present obvious sensitivity to hypoxia conditions.<sup>19-22</sup> For example, Thambi *et al.* grafted hydrophobic modified NI groups onto carboxymethyl dextran (CM-DeX) framework to prepare hypoxia-responsive nanoparticles (HR-NPs).<sup>19</sup> Deng *et al.* reported the copolymer self-assembled micelles by grafting the

aminated NI groups onto amphiphilic polymers, and achieved controllable drug release under hypoxic conditions.<sup>22</sup>

Recently, there are significant interests focused on the dual-stimuli-responsive polymers with a distinct opportunity to well adjust their responses to dual stimuli independently.<sup>23-33</sup> Dually responsive copolymers including temperature-pH dual responses<sup>34-36</sup>, temperature-glucose dual responses<sup>37-40</sup>, temperature-redox responses<sup>41-43</sup> had been reported, and the controlled release properties of these responsive polymeric systems were also proved. For example, Yuba *et al.* reported the pH-temperature dually responsive copolymer which could be modified on liposome surfaces for controlled cargo release.<sup>44</sup> Wang *et al.* reported the micelles assembled by using photo-temperature responsive copolymer for controlled-release under compound stimulation.<sup>45</sup> However, up to now, the dual-stimuli responsive polymers containing hypoxic response have rarely been reported. Therefore, it is necessary and worthwhile to investigate dual-response polymers with hypoxic response and other responses.

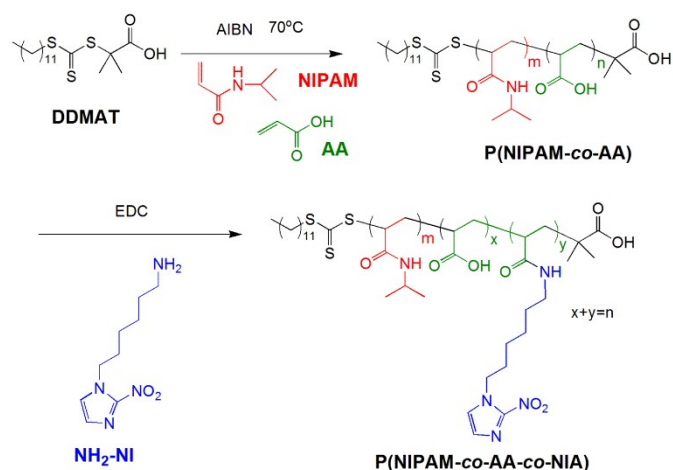
The change of temperature would lead to the morphological transformation of thermoresponsive polymeric self-assemblies.<sup>46-50</sup> In fact, temperature is one of the most controllable stimuli.<sup>51-55</sup> Among the temperature responsive polymers, poly(isopropylacrylamide) (PNIPAM) has been widely used as thermoresponsive materials in biomedical fields because its lower critical solution temperature (LCST) is close to human body temperature.<sup>56-60</sup> The PNIPAM segments can undergo a reversible phase transition accompanying with the swelling or shrinkage of structures, which endowed these polymers with potential application value in releasing drugs.<sup>61-66</sup> In addition, acrylic acid has been widely used in the field of

<sup>a</sup>Department of Interventional and Vascular surgery, Shanghai Tenth People's Hospital, School of Materials Science and Engineering, Tongji University, Shanghai 201804, People's Republic of China. E-mail: yuanwz@tongji.edu.cn (W. Yuan), Tel.: +86 21 69580234, Fax: +86 21 69584723.

<sup>b</sup>EYE & ENT Hospital of Fudan University, Shanghai 200031, People's Republic of China. E-mail: wuyongzhen\_fd@sina.com (Y. Wu)

biomedicine because of its good water solubility, biocompatibility and active chemical properties, which can be used for RAFT and EDC reactions.<sup>67, 68</sup>

Herein, the random copolymers of poly(isopropylacrylamide-co-acrylic acid-co-2-nitroimidazole acrylate) (P(NIPAM-co-AA-co-NIA)) with containing different amounts of NI group were synthesized by RAFT and EDC reactions (Scheme 1). The random copolymers could self-assemble in aqueous solution to form micelles. Under hypoxic conditions, the hydrophobic NI groups in P(NIPAM-co-AA-co-NIA) would be converted to hydrophilic 2-aminoimidazole (AI) groups through the catalytic action of reduced nicotinamide adenine dinucleotide phosphate (NADPH). Changes in hydrophilic properties of copolymers further induced the expansion of micelles or transformation into vesicles. In addition, the change of temperature also would alter the morphology of micelles. As a result, the P(NIPAM-co-AA-co-NIA) copolymer micelles could be used as a promising drug carrier to achieve the controlled release of doxorubicin (DOX), as shown in Fig. 1.



Scheme 1 Synthesis of P(NIPAM-co-AA-co-NIA) amphiphilic random copolymer by combining RAFT and EDC reactions.

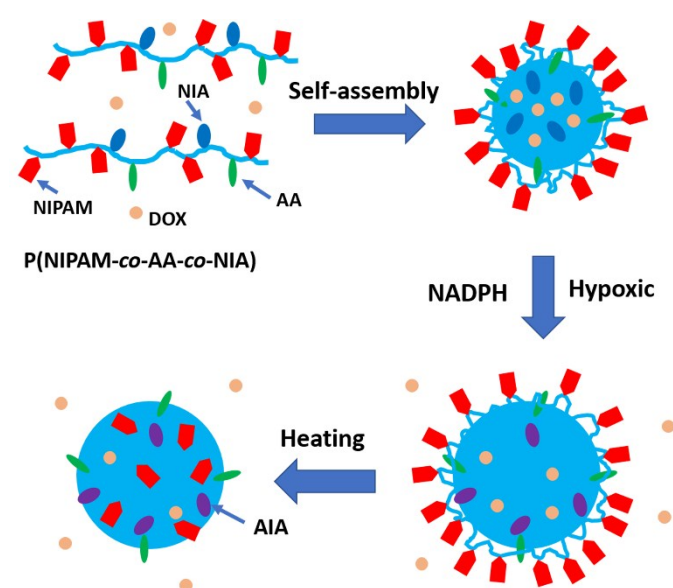


Fig. 1 Schematic illustration of the hypoxia and temperature responsive properties of P(NIPAM-co-AA-co-NIA) random copolymer micelles or vesicles and their controlled DOX release.

## Experimental

### Materials

2,2'-Azobisisobutyronitrile (AIBN, Aldrich, 98%) was recrystallized from ethanol. Acrylic acid (AA, Acros, 99.5%) was used directly without further purification. 2-nitroimidazole (NI, Adamas, 98%), Carbon disulfide (CS<sub>2</sub>, Adamas, 99.9%), 1-Dodecanethiol (C<sub>12</sub>H<sub>25</sub>SH, Adamas, 98%), Triethylamine (TEA, Adamas, 99.5%), N-hydroxysuccinimide (NHS, Adamas, 98%), N-boc-6-bromohexylamine (Energy Chemical, 98%) and 3-(3-dimethylaminopropyl)-1-ethylcarbodiimide hydrochloride (EDC-HCl, Adamas, 97%) were used as received. Aminated 2-nitroimidazole (NH<sub>2</sub>-NI) was synthesized by the reaction of NI, K<sub>2</sub>CO<sub>3</sub> and 6-(boc-amino)ethyl bromide according to the literature.<sup>19</sup> NIPAM was recrystallized from the toluene/hexane mixture (1:3).

### Characterizations

**Attenuated total reflection fourier transform infrared spectroscopy (ATR FT-IR).** An EQUINOSS/HYPERRION 2000 spectrometer (Bruker, Germany) was applied to collect ATR FT-IR spectra with a resolution of 1 cm<sup>-1</sup> from 650 to 4000 cm<sup>-1</sup> for 30 scans. Perkin Elmer Spectrum software was used for data acquisition and analysis.

**Proton nuclear magnetic resonance spectroscopy (<sup>1</sup>H NMR).** Bruker AVANCE-400 MHz NMR was used to obtain the <sup>1</sup>H NMR spectra of the synthesized polymers and modified hypoxic sensitive substance with CDCl<sub>3</sub> or DMSO-*d*<sub>6</sub> as the solvent.

**Gel permeation chromatography (GPC).** HLC-8320 (Tosoh, Japan) analysis system equipped with two columns (TSK gel super AWM-H×2, R0091+R0093) was used to obtain GPC data under a flow rate of 0.6 mL min<sup>-1</sup> at 40 °C by using DMF containing 10 mM LiBr as the eluent. The PMMA calibration kit was used as the calibration standard.

**UV-vis absorption spectroscopy.** The UV-vis absorption spectra were recorded on a UV-vis spectrophotometer (Lambda 35, PerkinElmer) with scanning rate of wavelength at 1 nm/s from 260 nm to 400 nm. Under hypoxic and normoxic conditions, the sample of the micelle solutions in a quartz cuvette was placed vertically under a high-pressure mercury lamp (wavelength 365 nm, power 200 W).

**Transmission electron microscopy (TEM).** The morphologies of the assembled micelles were observed on a JEOL JEM-2010 TEM at an acceleration voltage of 80 kV. The samples for observation were prepared by dropping a drop of assembled micellar solution on carbon coated copper grids and drying overnight before testing.

**Dynamic light scattering (DLS).** DLS were measured by using a Malven Autosizer 4700 DLS spectrometer to obtain the hydrodynamic radius (*R<sub>h</sub>*) value of the copolymer micelles. The scattering light was recorded at a fixed angle of 90° and the *R<sub>h</sub>* values were obtained by a cumulant analysis.

**Zeta potential.** ZETASIZER Nano series instrument (Malvern Instruments) was used to record the Zeta potential of self-assembled micelles under normoxic and hypoxic conditions.

### Synthesis of DDMAT

The chain transfer agent DDMAT was synthesized by using CS<sub>2</sub>, CHCl<sub>3</sub>, acetone, C<sub>12</sub>H<sub>25</sub>SH and NaOH. The specific procedures are as follows. Firstly, C<sub>12</sub>H<sub>25</sub>SH (48.46 g, 0.24 mol), (CH<sub>3</sub>)<sub>2</sub>CO (146.5 mL) and Aliquot 336 (3.90 g, 0.0096 mol) were added into a three-necked flask. After the system was cooled to 10 °C and filled with nitrogen. 50% NaOH solution (13.19 ml) was added dropwise into the mixed system and stirred for 20 min. Secondly, CS<sub>2</sub> (18.24 g, 0.24 mol) in acetone (30.74 mL) were added dropwise into the flask within 12 min, followed by the addition of CHCl<sub>3</sub> (28.8 mL). Add 50% NaOH solution (28.03 ml) dropwise into the system to conduct the reaction overnight. Thirdly, deionized water (360 mL) and hydrochloric acid (60 mL) were added into the mixture, followed by the rotary evaporation to remove acetone. Finally, the obtained mixture was filtered, recrystallized from *n*-hexane and dried for 24 h to obtain the orange solid.

<sup>1</sup>H NMR (CDCl<sub>3</sub>, δ, ppm): 11.0 (COOH), 1.62 (CH<sub>2</sub>CS and C(CH<sub>3</sub>)<sub>2</sub>), 1.28 (CH<sub>3</sub>(CH<sub>2</sub>)<sub>10</sub>), 0.82 (CCH<sub>3</sub>).

### Synthesis of P(NIPAM-co-AA)

P(NIPAM-co-AA) was synthesized by RAFT of AA and NIPAM with DDMAT as the chain transfer agent. Typically, NIPAM (5 g, 44.2 mmol), AA (1.6 g, 22.2 mmol), DDMAT (0.268 g, ), AIBN (12.1 mg, 0.074 mmol) and anhydrous DMF (8 mL) were added into the flask. After, repeating freeze-vacuum-charge argon for three times, the reaction was carried out at 70 °C under argon for 6-8 h. Thereafter, the resulting solution was added dropwise into ice-bathed *n*-hexane and then stayed overnight. Afterwards, the supernatant solution was removed and the final product was obtained after vacuum drying (yield: 93%).

$M_{n, NMR}=7826$  g/mol,  $M_{n, GPC}=7480$  g/mol,  $M_w/M_n=1.21$ . ATR FT-IR (cm<sup>-1</sup>): 3160-3700 (ν<sub>N-H</sub>), 1724 (ν<sub>C=O</sub>), 1647 (ν<sub>C=O</sub>), 1540 (ν<sub>C-N</sub>), 1381 (ν<sub>O-H</sub>). <sup>1</sup>H NMR (CDCl<sub>3</sub>, δ, ppm): 11.00 (-COOH), 8.00 (CNHC), 3.82 (NHCH), 3.38 (CH in PNIPAM), 1.28-2.20 (CH in PAA, CH<sub>2</sub> in PNIPAM and CH<sub>2</sub> in PAA, C(CH<sub>3</sub>)<sub>2</sub>CO in DDMAT), 1.06 (NHCH(CH<sub>3</sub>)<sub>2</sub> and C<sub>12</sub>H<sub>25</sub> in DDMAT).

### Synthesis of P(NIPAM-co-AA-co-NIA)

P(NIPAM-co-AA-co-NIA) random copolymers were synthesized by EDC reaction of P(NIPAM-co-AA) with different amounts of NH<sub>2</sub>-NI. The typical procedure is described as follows. P(NIPAM-co-AA) (0.5 g, 0.06 mmol) was dissolved in 12 mL of DMF, then EDC-HCl (3.21 g, 16.7 mmol) and NHS (1.93 g, 16.7 mmol) were added to obtain the solution via continuous stirring for 15 min. Afterthat, 8 mL DMF solution of NH<sub>2</sub>-NI (0.36 g, 1.7 mmol) was slowly added into the mixture to perform the reaction at room temperature for 24 h. The pure copolymers were obtained by dialyzing against methano/water mixing solvents (v<sub>1</sub>/v<sub>2</sub>=1/1) and deionized water respectively for 24 h and 48 h. The purified and dry product was obtained after freeze drying (yield: 89%).

$M_{n, NMR}=11516$  g/mol,  $M_{n, GPC}=10650$  g/mol,  $M_w/M_n=1.24$ . ATR FT-IR (cm<sup>-1</sup>): 3136-3706 (ν<sub>N-H</sub>), 1724 (ν<sub>C=O</sub>), 1641 (ν<sub>C=O</sub>), 1533 (ν<sub>C-N</sub>), 1420 (ν<sub>N=O</sub>), 1381 (ν<sub>O-H</sub>). <sup>1</sup>H NMR (DMSO-*d*<sub>6</sub>, δ, ppm): 7.16-7.67 (NCH=CHN), 3.82 (NHCH and NCH<sub>2</sub>C), 3.40 (CH in PNIPAM, NHCH<sub>2</sub>), 1.16-2.23 (CH<sub>2</sub> in PNIPAM, CH<sub>2</sub> and CH in PAA, C(CH<sub>3</sub>)<sub>2</sub>CO, C(CH<sub>2</sub>)<sub>4</sub>CNH), 1.06 (NHCH(CH<sub>3</sub>)<sub>2</sub> and C<sub>12</sub>H<sub>25</sub> in DDMAT).

**Micellization of P(NIPAM-co-AA-co-NIA) random copolymers**

Firstly, 50 mg of P(NIPAM-co-AA-co-NIA) copolymer was dissolved in 10 mL of DMF. Then, 20 ml deionized water was injected into the resulting solution by using a microinjection pump. Finally, the self-assembled micelles were formed by dialyzing the mixed solution against deionized water for 48 h using a dialysis membrane (molecular weight cut-off: 3500 Da), and the dialysis water was changed every 6 h.

### DOX loading and controlled release from micelles

The process for DOX loading was implemented as follows. Firstly, DOX-HCl (6 mg) and P(NIPAM-co-AA-co-NIA) (20 mg) were dissolved in 4 mL of DMF, then 0.6 mL of TEA was added into the mixture, followed by the continuous stirring for several minutes to form a homogeneous crimson solution. Then, the resulting solution was slowly added to 8 ml deionized water dropwise under ultrasonic treatment. After that, the system was sonicated for additional 30 min to obtain a purple-blue homogeneous solution. The solution was dialyzed against deionized water for 24 h using a dialysis membrane (molecular weight cut-off: 3500 Da), and the deionized water need to be refreshed every 2 h in the first 8 h and then every 6 h in later to remove the unloaded DOX molecules and organic solvents. Finally the dry micelles/vesicles loading DOX were obtained by freeze drying. The drug loading efficiency (DLE) and drug loading content (DLC) were calculated according to the following formulae:

### DOX loading and controlled release from micelles

DLC(wt%)= (weight of loading DOX/weight of DOX-loaded polymeric micelles )×100% (1)  
DLE(wt%)=(weight of loading DOX/weight of DOX in feed)×100% (2)

In the DOX release investigation, the freeze-dried DOX-loaded micelles were dispersed in PBS (pH=7.4) and transferred into a dialysis membrane (molecular weight cut-off: 3500 Da). For DOX release under hypoxic conditions, the dialysis membrane was immersed in the erlenmeyer flask filled with deoxidized PBS (pH=7.4) containing 100 mM NADPH which was continuously purged by using argon to maintain anaerobic condition. Then the flask was sealed and transferred into a 37 °C shaker with shaking at 150 rpm. 2.0 mL of release solution in the flask was collected for measurements and the equal volume of fresh PBS was replenished and the DOX concentration was obtained by measuring the extracted solution at 485 nm on a UV-vis spectrophotometer.

**In vitro cytotoxicity assay of copolymer micelles**

The 293T cells were used for investigating the cytotoxicities of the micelles or vesicles. In brief, the logarithmic 293T cells were seeded into a 96-well plate with the density of 5×10<sup>3</sup> cells per well, and the wells at edges were filled with sterile PBS. After that, the subject was incubated overnight at 37 °C humidified 5%

CO<sub>2</sub> condition with DMEM supplemental medium (containing 10% FBS) to ensure that the monolayer cells were covered the bottom of the well. Then, the cells were treated with different concentrations of pure and DOX loaded micelles/vesicles for 24 h. After removing the medium, MTT stock solution (20 μL, 5 mg/mL in PBS) was added into each well, followed by the incubation for another 4 h. Afterwards, the medium was sucked out carefully in each well and 150 μL of DMSO was added successively. The 96-well plate was transferred in a shaker with slight shaking for 10 min to ensure the complete dissolution of the intracellular MTT formazan crystals. Finally, a Multiscan MK3 plate reader was used to record the absorbance at 570 nm of the resulting solution. The relative cell viability can be calculated by the following formula:

$$\text{Relative cell viability \%} = (\text{OD}_{\text{treated}} / \text{OD}_{\text{control}}) \times 100$$

where OD<sub>treated</sub> was obtained from the presence of the micelles/vesicles and OD<sub>control</sub> was obtained from the absence of the micelles/vesicles.

## Results and discussion

### Synthesis of P(NIPAM-co-AA-co-NIA) random copolymers

The ATR FT-IR spectra of P(NIPAM-co-AA) and P(NIPAM-co-AA-co-NIA) were shown in Fig. S1. As shown in Fig. S1(a), the strong absorption peaks at 3160-3700 cm<sup>-1</sup> correspond to the N-H stretching vibration in the PNIPAM segment, while the strong absorption peak at 1647 cm<sup>-1</sup> is attributed to the C=O stretching vibration in the PNIPAM segment, and C-N stretching vibration peak appear at 1540 cm<sup>-1</sup>. These signals fully proved the successful polymerization of N-isopropylacrylamide monomer. Moreover, the characteristic group signal of PAA segment could also be detected by IR spectrum, the stretching vibration peaks of C=O and bending vibration peaks of O-H appeared at 1724 cm<sup>-1</sup> and 1381 cm<sup>-1</sup> respectively, indicating that acrylic monomers were successfully polymerized. Fig. S1(b) shows the ATR FT-IR spectrum of P(NIPAM-co-AA-co-NIA), in addition to the characteristic group signals in PNIPAM and PAA segments, the absorption peak at 1420 cm<sup>-1</sup> corresponded to N=O group, and the strengths of the stretching vibration peaks of C=O and bending vibration peaks of O-H in PAA segment decreased, which indicated that NI groups were successfully grafted onto the side chains of random copolymer P(NIPAM-co-AA). <sup>1</sup>H NMR spectra of DDMAT, P(NIPAM-co-AA) and P(NIPAM-co-AA-NIA) are shown in Fig. S2. <sup>1</sup>H NMR spectrum of DDMAT is shown in Fig. 2S(a). The proton of methyl-terminal can be detected at 0.82 ppm, the absorption peak at 1.28 ppm belonged to ten methylene's protons. Meanwhile, the proton peaks of methylene linked to C=S and two methyl linked to C-S appeared at 1.62 ppm, and the proton signal of carboxyl group appeared at 11.0 ppm. All these results proved the successful synthesis of DDMAT. <sup>1</sup>H NMR spectrum of P(NIPAM-co-AA) which was synthesized from N-isopropylacrylamide and acroleic acid monomer via RAFT, by using DDMAT as chain transfer and azodiisobutyronitrile as evocating agent was shown in Fig. S2(b). The proton signals of -NH group of PNIPAM chains and -COOH

group of PAA segment could be detected at 8.00 ppm and 11.00 ppm respectively, which confirmed the successful synthesis of P(NIPAM-co-AA). *M<sub>n,NMR</sub>* of P(NIPAM-co-AA) copolymer was calculated according to the integral ratio of corresponding peaks and the known molecular weight of PNIPAM and PAA blocks. The result was 7826 g/mol.

<sup>1</sup>H NMR spectrum of P(NIPAM-co-AA-co-NIA) shown in Fig. 2S(c) revealed the characteristic peaks of NI groups, which means the successful grafting of P(NIPAM-co-AA) and NH<sub>2</sub>-NI. Besides, the grafting number of NI group could be calculated from the integral ratio of the proton peak (k+1) in NI to the methyl proton peak ( $\frac{a}{a+m}$ ) in PNIPAM segment. The results indicated that the number of NI groups in copolymer was 19. Based on this result and *M<sub>n,NMR</sub>* of P(NIPAM-co-AA), the molecular weight of P(NIPAM-co-AA-co-NIA) was further calculated to be 11516 g/mol.

By controlling the feed ratio of NI and AA in copolymer, three kinds of P(NIPAM-co-AA-co-NIA) with different grafting numbers of NI groups were prepared. As shown in Table 1, the numbers of NI groups grafted to PAA segment are 8, 17 and 19 respectively. Namely, P(NIPAM<sub>48</sub>-co-AA<sub>18</sub>-co-NIA<sub>8</sub>), P(NIPAM<sub>48</sub>-co-AA<sub>9</sub>-co-NIA<sub>17</sub>) and P(NIPAM<sub>48</sub>-co-AA<sub>7</sub>-co-NIA<sub>19</sub>) have been successful synthesized.

**Table 1** Results of the random copolymers with different amount of NI groups

Sample	<i>M<sub>n,NMR</sub></i> (g/mol) <sup>a</sup>	<i>M<sub>n,GPC</sub></i> (g/mol) <sup>b</sup>	<i>M<sub>w</sub>/M<sub>n</sub></i> <sup>b</sup>
P(NIPAM <sub>48</sub> -co-AA <sub>18</sub> -co-NIA <sub>8</sub> )	9221	9012	1.12
P(NIPAM <sub>48</sub> -co-AA <sub>9</sub> -co-NIA <sub>17</sub> )	10967	9985	1.23
P(NIPAM <sub>48</sub> -co-AA <sub>7</sub> -co-NIA <sub>19</sub> )	11516	10650	1.24

<sup>a</sup> Determined by <sup>1</sup>H NMR spectroscopy of the random copolymers.

<sup>b</sup> Determined by GPC analysis with polystyrene standards. Use THF as eluent.

Fig. S3 showed the GPC curves of random copolymer P(NIPAM-co-AA-co-NIA), these curves are unimodal and symmetrical, indicating that the synthesized polymers are pure substances. The molecular weight and its distribution are shown in Table 1.

### Micellization of amphiphilic P(NIPAM-co-AA-co-NIA) random copolymers

To further explore the morphology and hydrodynamic radius of the micelles obtained by self-assembled amphiphilic copolymer P(NIPAM-co-AA-co-NIA), three polymer micelle samples with different grafting ratios of NI group were characterized by TEM and DLS respectively. The results are shown in Fig. 2.

The results of TEM characterization are shown in Fig. 2(a-c). The morphologies of micelles obtained by self-assembled P(NIPAM<sub>48</sub>-co-AA<sub>18</sub>-co-NIA<sub>8</sub>), P(NIPAM<sub>48</sub>-co-AA<sub>9</sub>-co-NIA<sub>17</sub>) and P(NIPAM<sub>48</sub>-co-AA<sub>7</sub>-co-NIA<sub>19</sub>) were regular spheres, which conformed the core-shell structure of amphiphilic molecule. In addition, the comparison among (a), (b) and (c) in Fig. 2 indicated that the size of micelles increased with the increasing graft number of NI groups in the copolymer. Fig. 2(a'-c') shows the hydrodynamic radius (*R<sub>h</sub>*) values of self-assembled P(NIPAM<sub>48</sub>-co-AA<sub>18</sub>-co-NIA<sub>8</sub>), P(NIPAM<sub>48</sub>-co-AA<sub>9</sub>-co-NIA<sub>17</sub>) and

P(NIPAM<sub>48</sub>-co-AA<sub>7</sub>-co-NIA<sub>19</sub>), respectively. Obviously, the change tendency of the hydrodynamic radius was similar to that displayed in TEM images. Namely, the  $R_h$  values increased from 63.7 nm, 85.1 nm to 101.8 nm with the increase of grafting number of NI groups. By comparing the results of the last two samples, while the grafting number of NI groups increased by only two, it was also caused a significant increase in  $R_h$  value, which was due to the increase of steric hindrance.

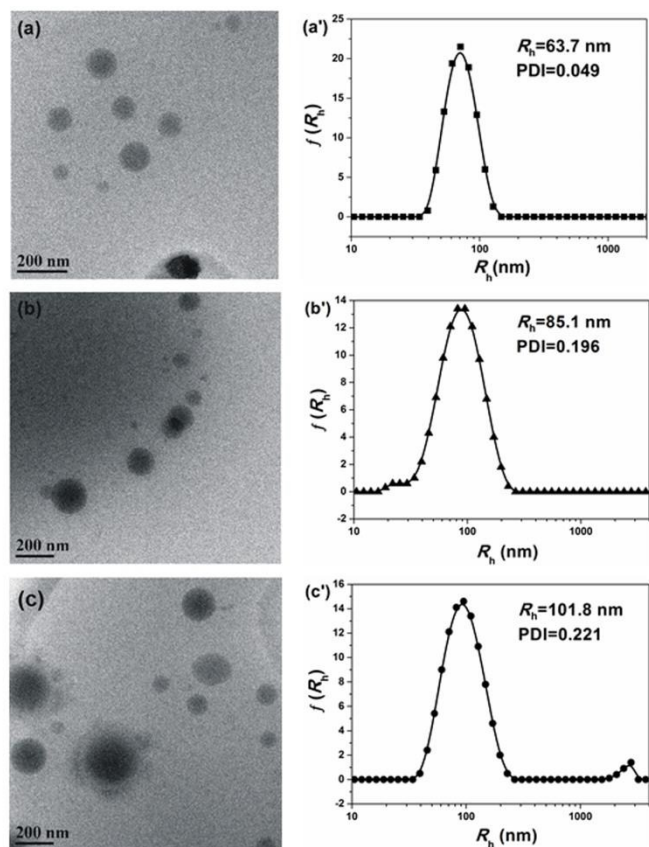


**Fig. 2** TEM images of (a) P(NIPAM<sub>48</sub>-co-AA<sub>18</sub>-co-NIA<sub>8</sub>), (b) P(NIPAM<sub>48</sub>-co-AA<sub>9</sub>-co-NIA<sub>17</sub>) and (c) P(NIPAM<sub>48</sub>-co-AA<sub>7</sub>-co-NIA<sub>19</sub>) and hydrodynamic radius ( $R_h$ ) of copolymer self-assemblies of (a') P(NIPAM<sub>48</sub>-co-AA<sub>18</sub>-co-NIA<sub>8</sub>), (b') P(NIPAM<sub>48</sub>-co-AA<sub>9</sub>-co-NIA<sub>17</sub>) and (c') P(NIPAM<sub>48</sub>-co-AA<sub>7</sub>-co-NIA<sub>19</sub>).

In addition, the  $R_h$  value of DLS was bigger than micellar radius obtained by TEM image, which was due to the fact that DLS test was for the micelle solution of polymer, including the thickness of hydration layer, but TEM test was for the morphology of dehydrated micelles. As a result, TEM test results were smaller than corresponding  $R_h$  values. To sum up, the increase trend of self-assembled micelles caused by the increased hydrophobicity of copolymers with the increase of the grafting NI groups number, which required more molecular to self-assembly into micelles. By designing polymers with different number of NI groups, more targeted biological applications can be achieved.

#### Hypoxia-responsive property of the random copolymer micelles

The performance of P(NIPAM-co-AA-co-NIA) random copolymer micelles in terms of hypoxic response was characterized and revealed by ultraviolet absorption measurement of the micelle

solutions from 260 nm to 400 nm. Micelle solutions were respectively treated under hypoxic (0.1% O<sub>2</sub>, 5% CO<sub>2</sub>) and normoxic (20% O<sub>2</sub>, 5% CO<sub>2</sub>) conditions, in PBS media containing NADPH (amount to the molar amount of nitro) at 37°C for 3 h. As revealed in Fig. 3a, the characteristic peak of NI group at 325 nm can be detected under normoxic conditions. Whereas, the peak of NI completely disappeared under hypoxic conditions, and a new peak appeared at 278 nm which was attributed to the characteristic peak of 2-aminoimidazole (AI), indicating that the conversion occurred from nitro group of NI to the amino group under hypoxic conditions. In the conversion progress, NADPH was acted as electron donor and transferred six electrons to catalyze the nitro groups. Furthermore, the intensities of peak were increased with the amount increase of AI groups in copolymer, correspondingly.

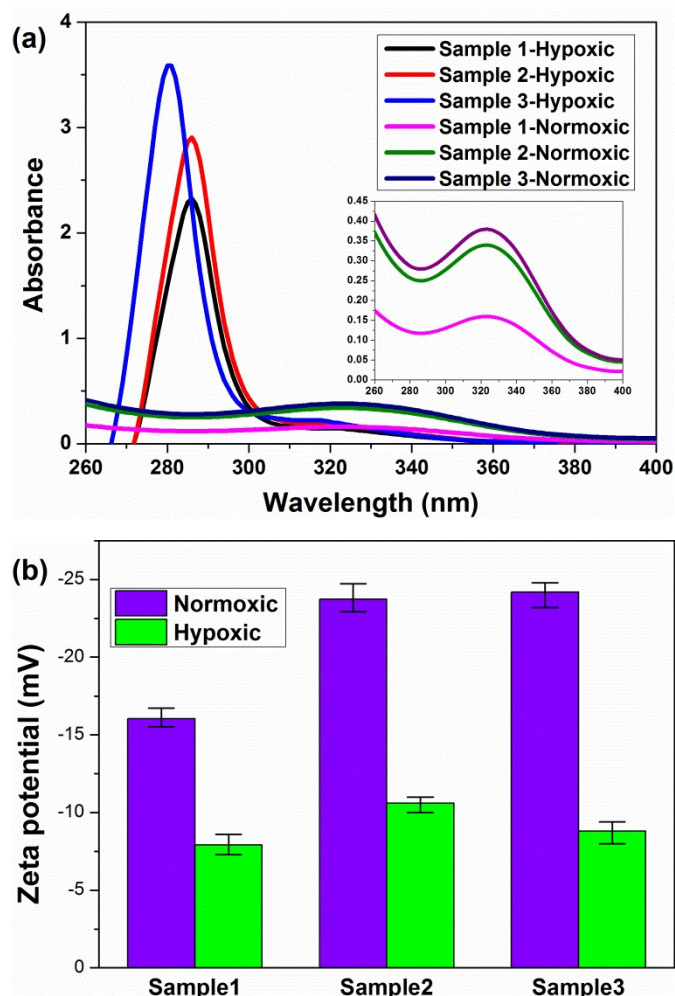


**Fig. 3** (a) UV absorption spectra of P(NIPAM<sub>48</sub>-co-AA<sub>18</sub>-co-NIA<sub>8</sub>) (Sample 1), P(NIPAM<sub>48</sub>-co-AA<sub>9</sub>-co-NIA<sub>17</sub>) (Sample 2) and P(NIPAM<sub>48</sub>-co-AA<sub>7</sub>-co-NIA<sub>19</sub>) (Sample 3) micelle solutions incubated for 3 h under normoxic and hypoxic conditions respectively. The samples were measured in PBS buffer containing 100 mM NADPH as electron donor. The illustration shows the conversion of NI into 2-aminoimidazole under hypoxic condition containing NADPH and (b) Zeta potential of P(NIPAM<sub>48</sub>-co-AA<sub>18</sub>-co-NIA<sub>8</sub>) (Sample 1), P(NIPAM<sub>48</sub>-co-AA<sub>9</sub>-co-NIA<sub>17</sub>) (Sample 2) and P(NIPAM<sub>48</sub>-co-AA<sub>7</sub>-co-NIA<sub>19</sub>) (Sample 3) micelle solutions incubated with 100 mM NADPH as electron donor under normoxic and hypoxic conditions.

The Zeta potential images of the P(NIPAM<sub>48</sub>-co-AA<sub>18</sub>-co-NIA<sub>8</sub>), P(NIPAM<sub>48</sub>-co-AA<sub>9</sub>-co-NIA<sub>17</sub>) and P(NIPAM<sub>48</sub>-co-AA<sub>7</sub>-co-NIA<sub>19</sub>) micelle

solutions are shown in Fig. 3b. The Zeta potentials of samples incubated with NADPH under normoxic conditions were -16.03 mV, -23.73 mV and -24.2 mV, respectively. After hypoxia treatment, the Zeta potentials of three copolymer micelles decreased rapidly to -7.90 mV, -10.59 mV and -8.80 mV, which was due to the change that the negatively charged nitro group of the NI was converted to positively charged amino group under anoxic circumstance with NADPH as electron donor. In addition, the absolute values of the decreased Zeta potentials were 8.13 mV, 13.14 mV and 15.4 mV respectively, which indicated that the increased content of NI group could enhance the hypoxic sensitivity of micelles.

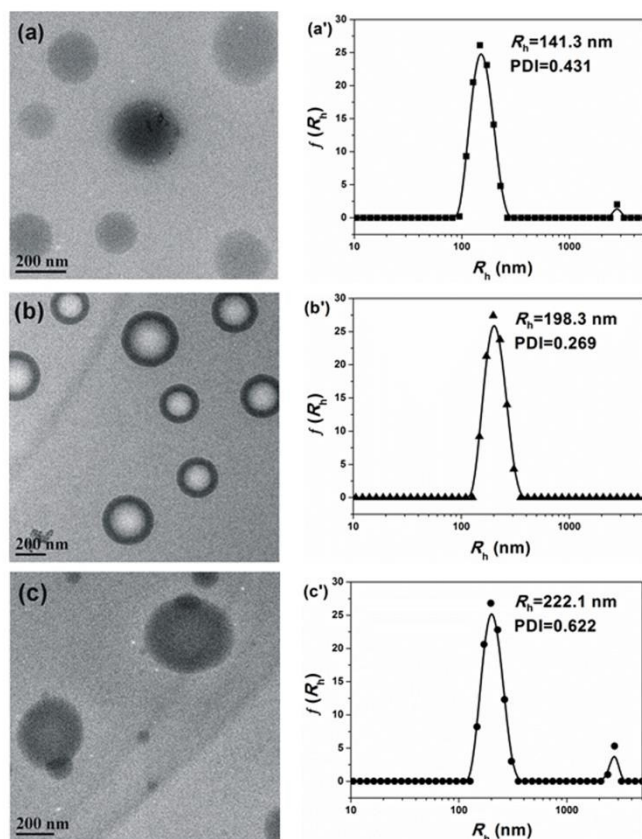


Fig. 4 TEM images of (a) P(NIPAM<sub>48</sub>-co-AA<sub>18</sub>-co-NIA<sub>8</sub>), (b) P(NIPAM<sub>48</sub>-co-AA<sub>9</sub>-co-NIA<sub>17</sub>) and (c) P(NIPAM<sub>48</sub>-co-AA<sub>7</sub>-co-NIA<sub>19</sub>) micellar and hydrodynamic radius ( $R_h$ ) of copolymer self-assemblies of (a') P(NIPAM<sub>48</sub>-co-AA<sub>18</sub>-co-NIA<sub>8</sub>), (b') P(NIPAM<sub>48</sub>-co-AA<sub>9</sub>-co-NIA<sub>17</sub>) and (c') P(NIPAM<sub>48</sub>-co-AA<sub>7</sub>-co-NIA<sub>19</sub>) after anoxic treatment.

The TEM and DLS characterizations of P(NIPAM<sub>48</sub>-co-AA<sub>18</sub>-co-NIA<sub>8</sub>), P(NIPAM<sub>48</sub>-co-AA<sub>9</sub>-co-NIA<sub>17</sub>) and P(NIPAM<sub>48</sub>-co-AA<sub>7</sub>-co-NIA<sub>19</sub>) after anoxic treatment are shown in Fig. 4. Compared with the image of micelles under normoxic conditions in Fig. 2, the copolymer micelles of P(NIPAM<sub>48</sub>-co-AA<sub>18</sub>-co-NIA<sub>8</sub>) and P(NIPAM<sub>48</sub>-co-AA<sub>9</sub>-co-NIA<sub>17</sub>) were still spherical but the radius increased obviously. For P(NIPAM<sub>48</sub>-co-AA<sub>7</sub>-co-NIA<sub>19</sub>), the micelles were transformed into vesicles with the increase of size, which can be attributed to the varying proportions of hydrophobic segments of the copolymer under hypoxic conditions. Fig. 4(a'-c') shows the variation in the  $R_h$  values of samples after anoxic treatment. Among them, the  $R_h$  values of copolymer micelles were 141.3 nm, 198.3 nm and 222.1 nm,

respectively. And the particle sizes obtained by DLS and TEM displayed the same change tendency, which can be attributed to the conversion from hydrophobic NI groups to hydrophilic AI groups catalyzed by NADPH under hypoxic conditions, leading to the expansion of micelles and even the structural change into vesicles like sample P(NIPAM<sub>48</sub>-co-AA<sub>7</sub>-co-NIA<sub>19</sub>). The morphological changes of micelles caused by their responsiveness indicated that it was possible to use them as smart carriers for drug targeting and controlled release.

#### Temperature-responsive property of the random copolymer micelles

The ultraviolet transmittance tests of P(NIPAM-co-AA-NIA) self-assembled micelles were carried out under different temperatures as shown in Fig. 5. The micelle solution was irradiated by ultraviolet light with wavelength of 500 nm from 20 °C to 56 °C, and the amplitude of variation was 0.5 °C per time. The ultraviolet transmittance of micelle solution was 50.2% at 20 °C. After that, with the increase of temperature, the ultraviolet transmittance decreased slightly in the temperatures ranging from 20 °C to 30 °C. When the temperatures ranged from 30 °C to 40 °C, the decrease in UV transmittance was accelerated. When the temperature increased up to 56 °C, the ultraviolet transmittance decreased slightly to the lowest value of 6.3%. The above results verified the temperature response property of copolymer P(NIPAM-co-AA-co-NIA), with the sensitive temperature ranges from 30 °C to 40 °C, which was similar to that of PNIPAM chain segment. The realization of temperature response property can be attributed to the morphological variation of the PNIPAM chain segment at the response temperature.

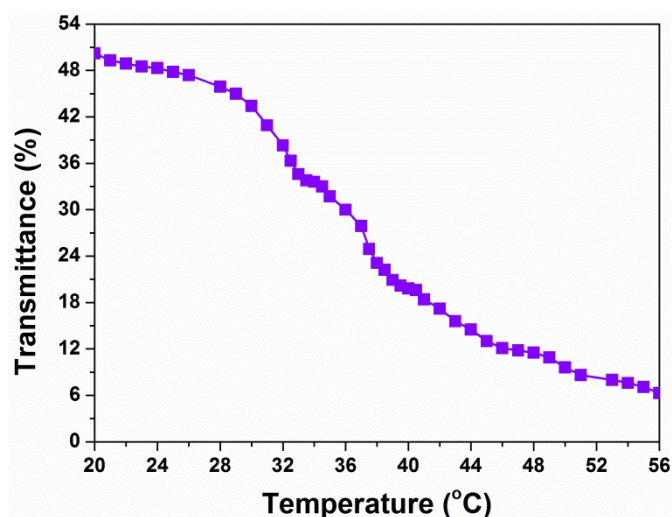


Fig. 5 Trend Diagram of UV transmittance of P(NIPAM<sub>48</sub>-co-AA<sub>7</sub>-co-NIA<sub>19</sub>) copolymer micelle with temperatures ranging from 20 °C to 56 °C.

The TEM images of P(NIPAM<sub>48</sub>-co-AA<sub>18</sub>-co-NIA<sub>8</sub>), P(NIPAM<sub>48</sub>-co-AA<sub>9</sub>-co-NIA<sub>17</sub>) and P(NIPAM<sub>48</sub>-co-AA<sub>7</sub>-co-NIA<sub>19</sub>) copolymer micelles after heating treatment under human body temperature (37 °C) and the  $R_h$  value of P(NIPAM<sub>48</sub>-co-AA<sub>7</sub>-co-NIA<sub>19</sub>) copolymer micelles with temperatures ranging from 25

°C to 50 °C have been recorded in Fig. 6. Obviously, the morphologies of micelle samples observed by TEM after heating treatment were no longer regular spherical, but were irregular small particles. Compared with Fig. 2, the size of each particle decreased, but the particles were aggregated together. As shown in Fig. 6d, the  $R_h$  value of self-assembled micelles was recorded at a scattering angle of 90° for each 1 °C. At temperature range from 25 °C to 33 °C,  $R_h$  decreased slightly. When the temperature exceeded above 33 °C, the  $R_h$  increased rapidly and continuously, which should be attributed to temperature responsiveness of the PNIPAM chain segment (LCST is 33 °C). With the increase of temperature below 33 °C, PNIPAM segments gradually became hydrophobic but not obviously, thus leading to the shrinkage of particle size. When the temperature was higher than LCST, the hydrophobic transformation occurred and led to aggregation of micelles into larger particle size.

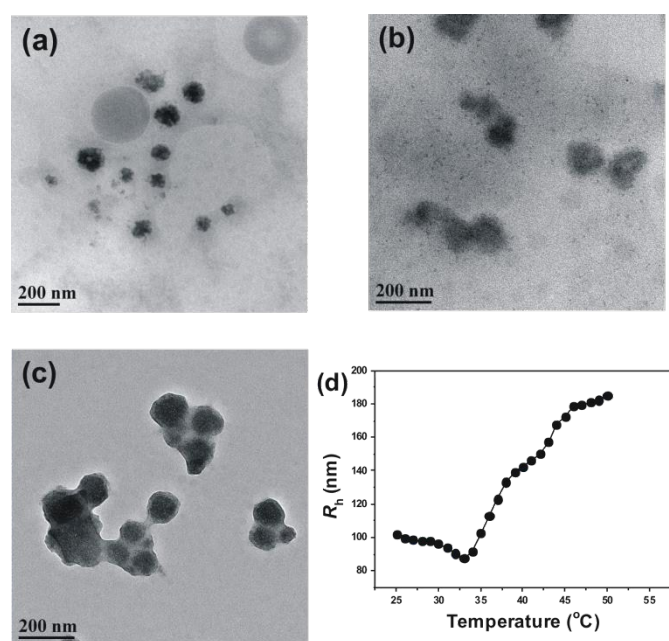


Fig. 6 TEM images of (a) P(NIPAM<sub>48</sub>-co-AA<sub>18</sub>-co-NIA<sub>8</sub>), (b) P(NIPAM<sub>48</sub>-co-AA<sub>9</sub>-co-NIA<sub>17</sub>) and (c) P(NIPAM<sub>48</sub>-co-AA<sub>7</sub>-co-NIA<sub>19</sub>) micellar after heating treatment under 37 °C and (d) trend diagram of hydrodynamic radius ( $R_h$ ) of P(NIPAM<sub>48</sub>-co-AA<sub>7</sub>-co-NIA<sub>19</sub>) with temperatures ranging from 25 °C to 50 °C.

#### *In vitro* cell assay and the controlled release of DOX

The *in vitro* cytotoxicity assays of micelles were carried out by using 293T cells after incubated at 37 °C for 24 h with copolymer micelles solution, and the cell viabilities were measured by MTT method. As shown in Fig. 7a, the cell viability was still up to 80% as the concentration of the copolymer micelles reached 100 mg/L, which indicated that the copolymer micelles had low cytotoxicity and good biocompatibility. In addition, Fig. 7b shows the cytotoxicities of Sample 3 loading DOX and free DOX under hypoxic and normoxic conditions. The free DOX exhibited the similarly strong cytotoxicities in both conditions. However, the cytotoxicity of DOX loaded copolymer micelles under hypoxic conditions was significantly higher than that under

normoxia conditions, which was due to the accelerated release of DOX under hypoxic conditions.

DOI: 10.1039/D0NJ02114H

Moreover, the IC<sub>50</sub> of DOX-loaded copolymer micelles can also be evaluated by the *in vitro* cell assay and the IC<sub>50</sub> for three samples were 4.16, 1.96 and 1.75 µg/L respectively, which can be seen in the Table 2.

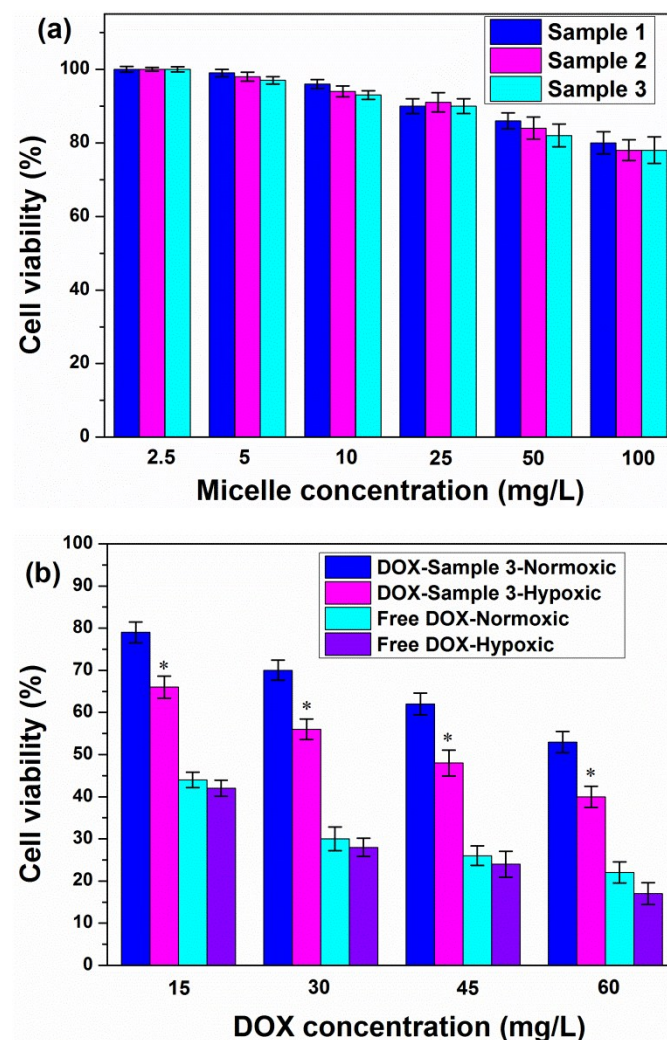


Fig. 7 (a) *In vitro* cytotoxicities of pure P(NIPAM<sub>48</sub>-co-AA<sub>18</sub>-co-NIA<sub>8</sub>) (Sample 1), P(NIPAM<sub>48</sub>-co-AA<sub>9</sub>-co-NIA<sub>17</sub>) (Sample 2) and P(NIPAM<sub>48</sub>-co-AA<sub>7</sub>-co-NIA<sub>19</sub>) (Sample 3) assembled micelles incubated with 293T cells for 24 h and (b) The cytotoxicities of DOX-loaded Sample 3 and free DOX incubated with 293T cells for 24 h under normoxic and hypoxic conditions with different concentration of DOX. Asterisks (\*) denote statistically significant differences ( $p < 0.05$  compared with DOX-loaded sample incubated under normoxic condition).

**Table 2** The IC<sub>50</sub> of three DOX-loaded polymeric micelles with different amount of NI groups<sup>a</sup>

Sample	IC <sub>50</sub> Micelle concentration (μg/L)
P(NIPAM <sub>48</sub> -co-AA <sub>18</sub> -co-NIMA <sub>8</sub> )	4.16
P(NIPAM <sub>48</sub> -co-AA <sub>9</sub> -co-NIMA <sub>17</sub> )	1.96
P(NIPAM <sub>48</sub> -co-AA <sub>7</sub> -co-NIMA <sub>19</sub> )	1.75

<sup>a</sup> The results determined by the *in vitro* cell assay experiments.

The drug-loading efficiency (DLE) of self-assembled micelles was 64.3% and the drug-loading content (DLC) was 8.39% which were calculated by formula (1) and (2) respectively.

In order to further study the effect of drug-loaded micelles on the controlled performance of drug release, the release experiments of DOX-loaded micelles were carried out under normoxic room temperature (23 °C), normoxic 37 °C and hypoxia 37 °C respectively. 2 mL of external PBS was taken out to determine the ultraviolet absorbance at 485 nm, and the cumulative drug release was calculated, as shown in Fig. 8. Obviously, under normoxic 23 °C conditions, the drug-loaded micelles could only release 24.61% of DOX after 24 h, and the release rate was slow. When the temperature was raised (37 °C), the rate of drug release in the first four hours was significantly increased, and the final drug release level was 35.49%. Therefore, it could be concluded that the temperature responsiveness of the copolymer micelles would lead to an increase in release rate and enhanced the drug-release capacity, that is, the temperature responsiveness facilitated the intelligent and controlled release of the copolymer micelles as drug carrier. Besides, under hypoxic conditions at 37 °C, the cumulative release level of DOX was significantly higher than that under normoxic conditions. After 10 h, the release rate was still fast, and the release level could reach 49.74 %. The final cumulative release level of drug-loaded micelles was 53.24 %, which was significantly higher than that under normoxic condition. The result further revealed that the conversion from the NI derivative to the AI derivative under hypoxic conditions could further promote DOX release. Compared with the single responsive self-assembled micelles in previous literature, the hypoxia and temperature dually responsive copolymer revealed stronger targeted drug delivery and more controllable release efficiency.<sup>17, 22, 69</sup>

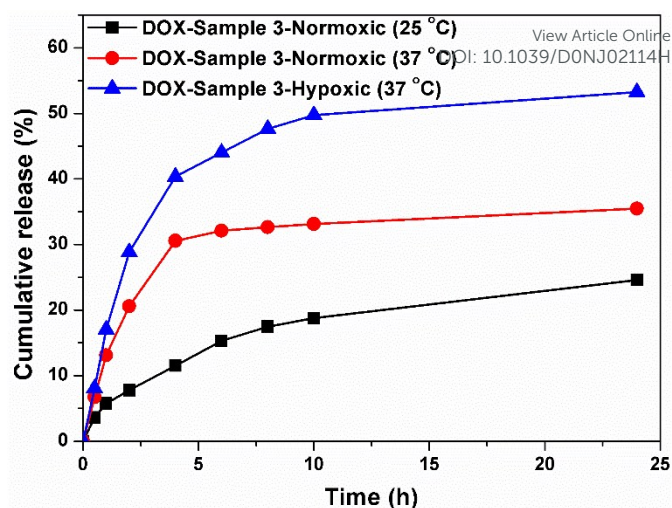


**Fig. 8** *In vitro* DOX release curves of P(NIPAM<sub>48</sub>-co-AA<sub>7</sub>-co-NIA<sub>19</sub>) (Sample 3) micelles under normal, hypoxic and heat conditions. Measurements were performed in PBS buffer (pH 7.4) containing 100 mM NADPH as reduction catalytic medium

## Conclusions

The amphiphilic copolymer P(NIPAM-co-AA-co-NIA) with both temperature and hypoxia responsiveness was successfully synthesized by RAFT and EDC reactions. By TEM, DLS and other characterizations, the copolymer assembled micelles exhibited a regular spherical shape with different sizes that closely related with the grafting rate of NI groups in copolymer. Meanwhile, by UV, DLS and Zeta etc., the P(NIPAM-co-AA-co-NIA) copolymer micelles under hypoxia conditions displayed the obviously hypoxic sensitivity, which was due to the hydrophilic transformation of NI groups. In addition, through the studies of TEM, UV transmittance and DLS in different temperatures, the morphology and hydrodynamic radius of micelles changed, indicating that the micelles possessed good temperature responsiveness. Furthermore, through *in vitro* cytotoxicity and cumulative release of drug-loaded micelles, it was found that the copolymer with biocompatible property could be used as a smart drug carrier to achieve the encapsulation and controlled release of hydrophobic drugs. In the double stimulation conditions of hypoxia and high temperature (37 °C), the cumulative release of drug was further enhanced and the release process was more controllable, thus verifying the potential for future applications in the biomedical field.

## Conflicts of interest

There are no conflicts to declare.

## Acknowledgements

The project was funded by the National Natural Science Foundation of China (no. 81771942).

## Notes and references

- 1 A. Ding, G. Lu, H. Guo and X. Huang, *Polym Chem*, 2017, **8**, 6997-7008.
- 2 Q. Chen, L. Feng, J. Liu, W. Zhu, Z. Dong, Y. Wu and Z. Liu, *Adv Mater*, 2016, **28**, 7129-7136.
- 3 C.-H. Luo, C.-T. Huang, C.-H. Su and C.-S. Yeh, *Nano Lett*, 2016, **16**, 3493-3499.
- 4 C. Qian, J. Yu, Y. Chen, Q. Hu, X. Xiao, W. Sun, C. Wang, P. Feng, Q.-D. Shen and Z. Gu, *Adv Mater*, 2016, **28**, 3313-3320.
- 5 A.-H. Rezaeian, C.-F. Li, C.-Y. Wu, X. Zhang, J. Delacerda, M. J. You, F. Han, Z. Cai, Y. S. Jeong, G. Jin, L. Phan, P.-C. Chou, M.-H. Lee, M.-C. Hung, D. Sarbassov and H.-K. Lin, *Nat Cell Biol*, 2017, **19**, 38-51.
- 6 G. L. Semenza, *Biochim Biophys Acta*, 2016, **1863**, 382-391.
- 7 R. Song, S. Peng, Q. Lin, M. Luo, H. Y. Chung, Y. Zhang and S. Yao, *Langmuir*, 2019, **35**, 10166-10172.
- 8 J. Yu, C. Qian, Y. Zhang, Z. Cui, Y. Zhu, Q. Shen, F. S. Ligler, J. B. Buse and Z. Gu, *Nano Lett*, 2017, **17**, 733-739.
- 9 J. Yu, Y. Zhang, Y. Ye, R. DiSanto, W. Sun, D. Ranson, F. S. Ligler, J. B. Buse and Z. Gu, *PNAS*, 2015, **112**, 8260-8265.
- 10 C. Zhao, N. Amiable, M. Laflamme, D. Marsolais, J. A. Di Battista, M. J. Fernandes and S. G. Bourgoïn, *Biochem Pharm*, 2019, **165**, 249-262.
- 11 K. Kiyose, K. Hanaoka, D. Oshiki, T. Nakamura, M. Kajimura, M. Suematsu, H. Nishimatsu, T. Yamane, T. Terai, Y. Hirata and T. Nagano, *J Am Chem Soc*, 2010, **132**, 15846-15848.
- 12 P. Kulkarni, M. K. Haldar, P. Katti, C. Dawes, S. You, Y. Choi and S. Mallik, *Bioconjugate Chem*, 2016, **27**, 1830-1838.
- 13 P. Kulkarni, M. K. Haldar, S. You, Y. Choi and S. Mallik, *Biomacromolecules*, 2016, **17**, 2507-2513.
- 14 F. Perche, S. Biswas, T. Wang, L. Zhu and V. P. Torchilin, *Angew Chem Int Ed*, 2014, **53**, 3362-3366.
- 15 J. Rao, C. Hottinger and A. Khan, *J Am Chem Soc*, 2014, **136**, 5872-5875.
- 16 J. V. E. Chan-Hyams, J. N. Copp, J. B. Smail, A. V. Patterson and D. F. Ackerley, *Biochem Pharm*, 2018, **158**, 192-200.
- 17 T. Thambi, V. G. Deepagan, H. Y. Yoon, H. S. Han, S.-H. Kim, S. Son, D.-G. Jo, C.-H. Ahn, Y. D. Suh, K. Kim, I. Chan Kwon, D. S. Lee and J. H. Park, *Biomaterials*, 2014, **35**, 1735-1743.
- 18 K. A. Krohn, J. M. Link and R. P. Mason, *J Nucl Med*, 2008, **49**, 1295-1485.
- 19 T. Thambi, S. Son, D. S. Lee and J. H. Park, *Acta Biomater*, 2016, **29**, 261-270.
- 20 F. Zhou, S. Zanganeh, I. Mohammad, C. Dietz, A. Abuteen, M. B. Smith and Q. Zhu, *Org Biomolecular Chem*, 2015, **13**, 11220-11227.
- 21 Z. Ahmad, S. Lv, Z. Tang, A. Shah and X. Chen, *J Biomater Sci Polym Ed*, 2015, **27**, 1-34.
- 22 Y. Deng, H. Yuan and W. Yuan, *J Mater Chem B*, 2018, **7**, 286-295.
- 23 Q. Wu, R. Wang, Y. Zhou, Y. Huang, R. Ghosh and X. Chen, *Chinese J Polym Sci*, 2015, **33**, 1048-1057.
- 24 M. Kurisawa and N. Yui, *J Control Release*, 1998, **54**, 191-200.
- 25 A. B. Siddique, J. W. An, H. J. Kim, H. Park, Y. J. Lee, G. C. Lee, H.-J. Kang, J. Y. Lee, S. Kim and J. Kim, *Macromol Res*, 2017, **25**, 70-78.
- 26 M. Zhou, K. Liu and X. Qian, *J Appl Polym Sci*, 2016, **133**, 43279.
- 27 M. L. Tebaldi, H. Charan, L. Mavliutova, A. Böker and U. Glebe, *Macromol Chem Phys*, 2017, **218**, 1600529.
- 28 X. Liu, H. Guo and L. Zha, *Polym Int*, 2012, **61**, 1144-1150.
- 29 H. Zou and H. Liu, *Int J Polym Mater Polym Biomater*, 2017, **66**, 955-962.
- 30 N. Morimoto, X.-P. Qiu, F. M. Winnik and K. Akiyoshi, *Macromolecules*, 2008, **41**, 5985-5987.
- 31 J. Jiang, D. Zhang, J. Yin and Z. Cui, *Soft Matter*, 2017, **13**, 6458-6464.
- 32 C.-W. Mao, R.-M. Wang, H.-F. Zhang, Y.-F. He, J.-D. Tao and X.-C. Ying, *J Control Release*, 2011, **152**, e68-e70.
- 33 J. Zhuang, M. R. Gordon, J. Ventura, L. Li and S. Thayumanavan, *Chem Soc Rev*, 2013, **42**, 7421-7435. DOI: 10.1039/DONJ02114H
- 34 Y. Wen and J. K. Oh, *Colloids Surf B: Biointerfaces*, 2015, **133**, 246-253.
- 35 Y. K. Kim, E.-J. Kim, J. H. Lim, H. K. Cho, W. J. Hong, H. H. Jeon and B. G. Chung, *Nanoscale Res Lett*, 2019, **14**, 77.
- 36 X. Zhang, C. Li, Y. Hu, R. Liu, L. He and S. Fang, *Polymer International*, 2014, **63**, 2030-2041.
- 37 P. Du, B. Mu, Y. Wang and P. Liu, *Mater Lett*, 2012, **75**, 77-79.
- 38 J. Li, L. Yang, X. Fan, J. Zhang, F. Wang and Z. Wang, *Int J Polym Mater Polym Biomater*, 2017, **66**, 577-587.
- 39 Y. Kotsuchibashi, R. V. C. Agustin, J.-Y. Lu, D. G. Hall and R. Narain, *ACS Macro Lett*, 2013, **2**, 260-264.
- 40 L. Sun, X. Zhang, C. Zheng, Z. Wu, X. Xia and C. Li, *RSC Adv*, 2012, **2**, 9904-9913.
- 41 H. Zou and W. Yuan, *J Mater Chem B*, 2014, **3**, 260-269.
- 42 Y.-K. Lin, Y.-C. Yu, S.-W. Wang and R.-S. Lee, *RSC Adv*, 2017, **7**, 43212-43226.
- 43 A. P. Vogt and B. S. Sumerlin, *Soft Matter*, 2009, **5**, 2347-2351.
- 44 T. Sugimoto, N. Yamazaki, T. Hayashi, E. Yuba, A. Harada, A. Kotaka, C. Shinde, T. Kumei, Y. Sumida, M. Fukushima, Y. Munekata, K. Maruyama and K. Kono, *Colloids Surf B: Biointerfaces*, 2017, **155**, 449-458.
- 45 F. Yang, Z. Cao and G. Wang, *Polym Chem*, 2015, **6**, 7995-8002.
- 46 S. R Sershen, S. L Westcott, N. Halas and J. L West, *J Biomed Mater Res*, 2000, **51**, 293-298.
- 47 J. Akimoto, M. Nakayama and T. Okano, *J Control Release*, 2014, **193**, 2-8.
- 48 X. Y. Xiong, K. C. Tam and L. H. Gan, *Polym*, 2005, **46**, 1841-1850.
- 49 E. Cyphert, H. A. von Recum, M. Yamato and M. Nakayama, *J Biomed Mater Res Part A*, 2018, **106**, 1552-1560.
- 50 Y.-I. Chen, C.-L. Peng, H.-J. Liu, P.-C. Lee, T.-Y. Luo and M.-J. Shieh, *Int J Nanomed*, 2016, **11**, 3357-3369.
- 51 D. Wang, Y. Jin, X. Zhu and D. Yan, *Prog Polym Sci*, 2017, **64**, 114-153.
- 52 H. Hayashi, K. Kono and T. Takagishi, *Bioch Biophys Acta-Biomembranes*, 1996, **1280**, 127-134.
- 53 M. Okubo, H. Ahmad and T. Suzuki, *Colloid Polym Sci*, 1998, **276**, 470-475.
- 54 B. P. Koppolu, Z. Bhavsar, A. Wadajkar, S. Nattama, M. Rahimi, F. Nwariaku and K. Nguyen, *J Biomed Nanotech*, 2012, **8**, 983-990.
- 55 R. Suedee, V. Seechamnaturakit, B. Canyuk, C. Ovatlarnporn and G. P. Martin, *J Chromatogr A*, 2006, **1114**, 239-249.
- 56 X. Z. Zhang and R. X. Zhuo, *Macromol Chem Phys*, 1999, **200**, 2602-2605.
- 57 W. Liu, B. Zhang, W. W. Lu, X. Li, D. Zhu, K. De Yao, Q. Wang, C. Zhao and C. Wang, *Biomaterials*, 2004, **25**, 3005-3012.
- 58 B. P. Koppolu, A. Wadajkar, M. Rahimi and K. Nguyen, *J Nanoparticle Research*, 2008, **11**, 1375-1382.
- 59 X. Chen, H. Song, T. Fang, J. Bai, J. Xiong and H. Ying, *J Appl Polym Sci*, 2010, **116**, 1342-1347.
- 60 S.-Q. Liu, Y.-Y. Yang, X.-M. Liu and Y.-W. Tong, *Biomacromolecules*, 2003, **4**, 1784-1793.
- 61 B. Sierra-Martin, J. R. Retama, M. Laurenti, A. Fernández Barbero and E. López Cabarcos, *Adv Colloid Interface Sci*, 2014, **205**, 113-123.
- 62 B. R. Saunders, N. Laajam, E. Daly, S. Teow, X. Hu and R. Stepto, *Adv Colloid Interface Sci*, 2009, **147-148**, 251-262.
- 63 A. Fernández-Barbero, I. J. Suárez, B. Sierra-Martín, A. Fernández-Nieves, F. J. de las Nieves, M. Marquez, J. Rubio-Retama and E. López-Cabarcos, *Adv Colloid Interface Sci*, 2009, **147-148**, 88-108.
- 64 K. Kratz, T. Hellweg and W. Eimer, *Polym*, 2001, **42**, 6631-6639.
- 65 K. Kratz and W. Eimer, *Ber Bunsenges Phys Chem*, 1998, **102**, 848-854.

ARTICLE

Journal Name

66 K. Kratz, T. Hellweg and W. Eimer, *Ber Bunsenges Phys Chem*, 1998, **102**, 1603-1608.  
 67 Y. Zhao, Y. Li, J. Ge, N. Li and L.-B. Li, *Drug Dev Ind Pharm*, 2013, **40**, 1483-1493.  
 68 S. W. Hong, K. H. Kim, J. Huh, C.-H. Ahn and W. H. Jo, *Macromol Res*, 2005, **13**, 397-402.  
 69 C.-L. Peng, Y.-I. Chen, H.-J. Liu, P.-C. Lee, T.-Y. Luo and M.-J. Shieh, *Inter J Nanomed*, 2016, **11**, 3357-3369.

View Article Online  
 DOI: 10.1039/D0NJ02114H

New Journal of Chemistry Accepted Manuscript

Downloaded from https://pubs.rsc.org on 19 May 2020 at 18:21:21

## TOC

The micelles self-assembled from P(NIPAM-co-AA-co-NIA) copolymers presented hypoxia and temperature dual responsive properties and achieve the controlled release of drug.

